Comment on the article “Parametric Instability Induced by X-Mode Wave Heating at EISCAT” by Wang et al. (2016)

N. F. Blagoveshchenskaya [1], T. D. Borisova [1], T. K. Yeoman [2]

[1] Department of Geophysics, Arctic and Antarctic Research Institute, St. Petersburg, 199397, Russia

[2] University of Leicester, Department of Physics and Astronomy, Leicester LE1 7RH, UK

Abstract. In their recent article Wang et al. [2016] analyzed observations from EISCAT (European Incoherent Scatter Scientific Association) Russian X-mode heating experiments and claimed to explain the potential mechanisms for parametric decay instability (PDI) and oscillating two-stream instability (OTSI) and to understand the physical factors accounting for parametric instability generated by an X-mode HF pump wave. Wang et al. [2016] claim that they cannot separate the HF-enhanced plasma and ion lines (HFPLs and HFILs) excited by O- or X-mode in the EISCAT UHF radar spectra due to an inability to distinguish the parametric instability excited by O- /X-mode heating waves according to their different excitation heights. Their reflection heights were determined from ionosonde records between the heater pulses which provide a rough measure of excitation altitudes and cannot be used for the separation of the O- and X-mode effects. The serious limitation in their analysis and interpretation of the PDI/OTSI is the use of a 30 s integration time of the UHF radar data. There are also serious disagreements between their analysis and the real observational facts. The fact is that it is the radical difference in the behavior of the X- and O-mode plasma and ion line spectra derived with 5 s resolution which provides the correct separation of the X- and O-mode effects. Although Wang et al. (2016) claim to derive the threshold of the parallel electric field for the PDI and OTSI, it would only hold for the classic resonance PDI and OTSI excited as immediate response to the onset of heating and is typical only for O-mode pumping at $f_H \leq foF2$. It is not discussed and explained how the parallel component of the electric field under X-mode heating is generated. Apart from the leakage to O-mode, results by Wang et al. [2016] do not explain the potential mechanisms for PDI and OTSI and add nothing to understanding the physical factors accounting for parametric instability generated by an X-mode HF pump wave.

1. Introduction

The growing body of X-mode experiments at the EISCAT (European Incoherent Scatter Scientific Association) HF heating facility with the use of various multi-instrument diagnostics showed that extraordinary (X-mode) powerful HF radio waves are capable of producing a strong modification of the high latitudinal ionospheric F-region, including the generation of the artificial field-aligned irregularities (FAIs) [*Blagoveshchenskaya et al.*, 2011a; b; 2013], optical emissions at red (630 nm) and green (557.7 nm) lines [*Blagoveshchenskaya et al.*, 2014], various spectral components in the narrowband SEE (stimulated electromagnetic emission) spectra [*Blagoveshchenskaya et al.*, 2015]. Considerable study has been given to the HF-enhanced ion and plasma lines (HFILs and HFPLs) from the EISCAT UHF radar spectra excited under X-mode heating, which are the signatures of the ion acoustic and Langmuir electrostatic waves) [*Blagoveshchenskaya et al.*, 2014; 2015]. This is evidence for the generation of the parametric decay instability (PDI). The appearance of a nonshifted component in the ion line spectrum is indicative of the excitation of the oscillating two- stream instability (OTSI). It was also found that, generally, the X-mode HFILs and HFPLs demonstrate similar behavior and features in the overdense and underdense ionosphere (when the pump frequency is below and above the critical frequency foF2) [*Blagoveshchenskaya et al.*, 2014; 2015]. It is significant that all the X-mode phenomena mentioned above are only excited when the extraordinary HF pump wave is radiated towards the magnetic zenith [*Blagoveshchenskaya et al.*, 2015].

Some theoretical investigations, related to the excitation of parametric instabilities by the X-mode waves have been carried out. *Fejer and Leer* [1972] suggested that parametric electromagnetic instability could be excited when the HF pump wave has extraordinary polarization. Here the exciting wave has an extraordinary polarization and the excited high frequency wave has the ordinary polarization. Both are electromagnetic waves in this case. *Vas'kov and Ryabova* [1998] proposed that extraordinary HF heating wave can generate the

upper hybrid (UH) waves as well as enhancements of low frequency plasma waves as a result of pump-induced scattering by ions. *Fejer and Leer* [1972] demonstrated that an X-mode pump wave is capable of exciting electrostatic waves in the Bernstein mode whose propagation vector is normal to the external magnetic field and whose frequency is that of the incident wave. Further, *Sharma et al*. [1994] proposed the parametric decay instability of X-mode heating waves into electrostatic electron Bernstein (EB) and ion Bernstein (IB) waves.

In their recent article Wang et al. [2016], from now called on WANG2016, claim to investigate the potential mechanisms and to understand the physical factors accounting for parametric decay instability (PDI) and oscillating two-stream instability (OTSI) generated by an X-mode HF pump wave by analyzing the HF-enhanced ion and plasma lines (HFILs and HFPLs) from EISCAT UHF radar observations. For this purpose they used the UHF incoherent scatter radar observations obtained in the course of three Russian EISCAT X-mode heating experiments on October 19, 2012, February 21 and October 22, 2013. WANG2016 distinguished the O- and X-mode parametric instability in accordance with the different reflection altitudes of the O- and X-mode HF pump wave. Their reflection heights were determined from ionosonde observations (ionograms) between heater pulses. The threshold electric field for the parametric decay instability excited by an X-mode pump wave is also investigated and compared with the experimental observations.

In this comment we demonstrate that analysis and interpretation of our EISCAT heating experiments described by WANG2016 is flawed. We also show that the separation of O- and X mode effects used by WANG2016 is incorrect. The separation of the O- and X-mode effects plays a crucial role in further analysis of the PDI and OTSI. The subsequent analysis by WANG2016 fails if such separation is incorrect. We present the separation procedure of the HF-induced ion and plasma lines excited by the X-and O-mode pump waves based on the specific features and distinctions between the UHF radar spectra. Then we briefly analyze the UHF radar observations in the course of O/X mode Russian EISCAT HF heating experiments described by WANG2016 with the use of the proposed UHF radar spectra separation. We then review WANG2016 step by

step to disclose the flaws and failures of their analysis of observations, separation of the O-and X-mode effects, and analysis of parametric decay instability excited by the extraordinary HF pump wave.

2. The separation of the X- and O-mode effects from EISCAT UHF radar spectra

Below we present experimental results showing the distinctive features and behaviors of HF-enhanced ion and plasma lines (HFILs and HFPLs) induced by extraordinary and ordinary polarized HF pump waves in the course of our experiment on February 21, 2013 (case 3 by WANG2016). An overview of phenomena from the EISCAT UHF radar observations in the course of an alternating O/X-mode heating experiment on February 21, 2013 from 12.12 to 14.30 UT is shown in Figure 1. Remember that HF pumping was produced towards the magnetic zenith with the effective radiated power of about 530 MW at heater frequency of 7.1 MHz with alternating O/X-mode polarization. In the course of the experiment the heater frequency was near or just above the critical frequency of the F2 layer. Fig. 1 illustrates the behavior of electron density and temperature (Ne and Te), undecoded downshifted plasma line power, and backscatter power (labeled as raw electron density) obtained from “raw” radar data with 30 s integration time. As seen from Fig. 1, strong backscatter power (the bottom panel), which points to the excitation of HF-enhanced ion lines, was observed in all O- and X- mode transmission pulses with the exception the last X-mode pulse from 14:16 – 14:26 UT, when fof2 quickly dropped. From ionosonde records which were used for the separation of the O-and X-mode effects in all analyzed cases, WANG2016 concluded that O-mode pump wave is not reflected from the ionosphere from 12:01 UT to 14:26 UT.

The excitation of X-mode HFILs was accompanied by strong HF-enhanced downshifted plasma lines observed throughout the whole heating pulse. The other situation was realized for

O-mode cycles, in which the excitation of HFPLs took place only as response to the heater turn on in cycles from 12:31 – 12:41 and 13:01 – 13:11 UT. In the course of O-mode cycles from 13:31 – 13:41 UT and 14:01 -14:11 UT, HFPLs were observed sporadically. Here the HF heating wave starts partly to penetrate out the ionosphere that leads to strong and specific effects in the HFILs behavior and sporadic appearance of HFPLs. In fact, the experiment on February 21, 2013 is not typical at all, as WANG2016 concluded. Moreover, this experiment is not typical even in the stable ionosphere from 12:10 to 13:30 UT. As seen from Fig. 1, the altitude of the X-mode HFILs was higher than the altitude of appearance of the O-mode HFILs throughout the time interval from 12:10 to 13:30 UT. Note, that we did not analyze the first O-mode pulse from12:01 – 12:11 UT owing to tuning up the HF heater at Tromsø.

Further we present results of the analysis in detail and comparison between the plasma and ion line spectra derived from “raw” UHF radar data with 5 s time resolution, excited by O- and X-mode heating wave for experiment on February 21, 2013. We have chosen and compared two consecutive heater pulses at heater frequency f_H = 7.1 MHz from 12:46 – 12:12.56 UT (X-mode) and 13:01 – 13:11 UT (O-mode) and at f_H = 5.423 MHz from 14:31 – 14:41 (O-mode) and 14:46 – 14:56 UT (X-mode). The main attention is paid to the growth time of HFPLs and HFILs after the heater is turned on. Figure 2 shows the behavior of maximum power of HF-enhanced downshifted plasma lines and upshifted and downshifted ion lines (on a logarithmic scale) on February 21, 2013 at fixed altitudes during 30 s before and 2 min after the heater onset for O- and X-mode heating at frequencies of 7.1 MHz (Fig. 2a) and 5.423 MHz (Fig. 2b). The power of the HFPLs and HFILs was found as the maximum in spectra derived every 5 s with 3 km altitude steps.

From Fig. 2a it is clearly seen that the turn on of the ordinary polarized HF pump wave at frequency of 7.1 MHz is accompanied by the abrupt increase of the intensity of the downshifted plasma line (HFPL) and upshifted and downshifted ion lines ($HFIL_{UP}$ and $HFIL_{DOWN}$). They reached the maximum in the first 5 s data dump and then decay in the next few data dumps. It is

141 the classic signature of the resonance parametric decay instability (PDI) [*Perkins et al*., 1974;
142 *Fejer*, 1979; *Hagfors et al*., 1983; *DuBois et al*., 1990; *Stubbe et al*., 1992; *Gurevich et al*., 2004;
143 *Kuo*, 2015] when the O-mode HF pump wave decays into the Langmuir and ion-acoustic waves
144 near the reflection height of O-mode wave. PDI develops from the "cold" start, acts over few
145 milliseconds of heating and can be recognized in the EISCAT UHF radar spectra in the first few
146 5s data dumps as HF-enhanced plasma and ion lines (initial overshoots) [*Robinson*, 1989].
147 Thereafter Langmuir and ion-acoustic waves are normally quenched by fully generated artificial
148 small-scale field-aligned irregularities (FAIs) preventing further generation of the PDI [*Stubbe*,
149 1996]. However, under high effective radiated power, the reappearance of enhanced ion and
150 plasma lines can occur after overshoots [*Dhillon and Robinson*, 2005; *Mishin et al*., 2016]. Such
151 a situation was observed during the O-mode pump pulse at f_H = 7.1 MHz when HF-enhanced
152 upshifted and downshifted ion lines reappeared (see Fig. 2a, top panel).
153 Behaviour of the enhanced plasma and ion line backscatters for X-mode pulse at f_H = 7.1
154 MHz differs radically from the O-mode one. As seen from Fig. 2a (bottom panel), HF-enhanced
155 plasma and ion lines appeared not from the "cold" start, that is observed for O-mode, but 15 s
156 later. Thereafter their power was gradually increased reaching a maximum within about 1 min.
157 The analogous behaviour of the HF-enhanced ion and plasma line power was observed
158 for O- and X-mode heating pulses at heater frequency of 5.423 MHz (see Figure 2b). An
159 important point is that the heater frequency f_H = 5.423 MHz is close the fourth electron gyro-
160 harmonic frequency, in the vicinity of which FAIs are suppressed. This results in the HF-
161 enhanced plasma and ion lines being quenched by FAIs to a smaller degree [*Stubbe*, 1996]. This
162 is clearly seen from the behaviour of HF-enhanced upshifted and downshifted ion lines (see Fig.
163 2b, top panel). As for X-mode pulse (fig. 2b, bottom panel), the enhanced plasma and ion lines
164 appeared with time delay of about 1 min after the heater is turned on (T_0). Thereafter they
165 gradually increased reaching a maximum after 2 min from T_0.

Let's further consider the plasma and ion line spectra for O- and X-mode heating which were derived from raw EISCAT UHF radar data at five fixed altitudes with 5 s resolution. Figures 3 and 4 show the downshifted plasma line spectra and ion line spectra at 5 altitudes for different times after the heater onset taken on February 21, 2013 at heater frequency f_H = 7.1 MHz for the same the O- and X-mode heating pulses as in Fig. 2a. Fig. 3a and b illustrate plasma line spectra for O-and X-mode pulses respectively and Fig. 4a and b depict ion line spectra.

The intense downshifted plasma line spectrum appeared as immediate response to the O-mode pump onset and was seen in the first 5 s UHF radar data dump (13:01:05 UT). It possess the sharp peak shifted by the ion-acoustic frequency ("mother" Langmuir wave) and three intense downshifted cascade lines, so called "daughter" Langmuir waves. In the next two 5 s dumps the O-mode plasma line spectra decayed and moved to a lower altitude.

An X-mode downshifted plasma line spectrum appeared within 15 s after the onset of HF pumping at an altitude of 225 km, which is 3 km higher as compared with the initial appearance of O-mode enhanced plasma lines. Then the intensity of plasma line spectra gradually increased and reached the maximum at 12:47:40 UT (after 100 s of HF pumping). At 12:48:50 UT the most intense plasma line spectrum moved to 228 km. Not too strong cascade lines in the X-mode plasma line spectra can be also recognized.

O-mode ion line spectra (Fig. 4a), similar to the downshifted plasma line spectra, initially appeared at 13:01:05 UT in the first 5 s UHF radar data dump. They possess a strong peak at zero frequency and two intense shoulders, upshifted and downshifted from zero frequency by the ion-acoustic frequency. The presence of the peak at zero frequency in the UHF radar ion line spectrum indicates the excitation of oscillating two-stream instability (OTSI) [*Kuo et al*., 1997]. Thereafter the ion line backscatter moved to lower altitudes from 225 km at 13:01:05 UT to 207 km at 13:01:50 UT, but its intensity was less as compared with the HF pump onset. Such descending ion line backscatter under O-mode heating was often observed at EISCAT/Heating facility and HAARP [*Dhillon and Robinson,* 2005; *Ashrafi et al., 2007*; *Mishin et al*.,

2016].Notice that from 13:01:50 UT the ion line spectra appeared also at an altitude of 204 km (not shown in Fig. 4a). From 13:02:10 UT their intensity was approximately the same as at 207 km. Ion line spectra were observed throughout the whole O-mode pump pulse.

An X-mode ion line backscatter developed at 12:46:15 UT within 15 s after the onset of HF pumping (see Fig.4b). The spectra exhibit only upshifted shoulders at altitudes of 219, 222, and 225 km (with the maximum at 222 km) and only downshifted shoulders at 207 km. Thereafter their intensity gradually increased at altitudes of 222 and 225 km. From 12:46:35 UT the most intense ion line backscatter shifted 3 km higher to 225 km which is the altitude of initial excitation of ion-acoustic waves under the O-mode heating (see Fig. 4a). After 70 s pumping (12:47:10 UT) ion line spectra at 222 and 225 km possess upshifted and downshifted shoulders together with weak zero component. The intensity of the ion line spectra, similar to the plasma line spectra, reached the maximum at 12:47:40 UT (after 100 s of HF pumping).

Figures 5 and 6 present the downshifted plasma line spectra and ion line spectra at five altitudes for different times after the onset of HF pumping taken on February 21, 2013 at heater frequency f_H = 5.423 MHz for the same O- and X-mode pulses as in Fig. 2b. Spectra are shown in the same manner as in Fig. 3 and 4. As a whole, the distinctive features and behavior at times of O- and X-mode plasma and ion line spectra are similar to those observed at heater frequency f_H = 7.1 MHz. Namely, strongly enhanced ion and plasma line spectra under O-mode HF pumping appeared from the “cold” start immediately after the onset of HF heating and were seen in the first 5 s radar data dump. Thereafter the ion line backscatter layer descended to lower altitudes. The persistent O-mode ion line backscatter was observed both at f_H = 7.1 MHz and f_H = 5.423 MHz.

The X-mode ion and plasma lines developed with a time delay relatively to the onset of HF heating. After appearance, their intensity gradually increased. However, there are some specific features at the pump frequency f_H = 5.423 MHz as compared with the 7.1 MHz case. The strength of the ion line spectra did not decay too much through the O-mode heating pulse.

This is explained by the proximity of the pump frequency to the fourth electron gyro-harmonic frequency, where FAIs are suppressed and ion lines are quenched to a smaller degree. As for the X-mode pulses, HF-enhanced ion and plasma lines developed after much longer delay time of about 60 s. The X-mode plasma and ion line spectra exhibit a very strong zero component, pointing to the OTSI excitation.

We have also considered the behavior and features of plasma and ion line spectra derived from the EISCAT UHF "raw" data with 5 s temporal resolution on October 22, 2013 (case 1 from WANG2016). As example, Figure 7 presents the downshifted plasma line spectra (a) and ion line spectra (b) at five altitudes for different times after the onset of pumping taken at heater frequency f_H = 7.1 MHz for the X-mode pulse from 16:01 – 16:11 UT. As seen from Fig. 7, the plasma and ion line spectra clearly revealed features typical for X-, but not for O-mode pumping. Their intensities gradually increased and reached a maximum at 16:01:50 UT within 50 s after the heater on, while in the course of O-mode heating the strongly enhanced ion and plasma line spectra appeared from the "cold" start in the first 5 s radar data dump. The specific feature in the behavior of ion line spectra was the presence of two maxima at different altitudes in the downshifted ion line intensities (see Fig. 7b). The first maximum is located at 228 km and the second one is at a height of 237 km. The same feature was often observed in a large body of X-mode experiments carried out at pump frequencies both below the critical frequency of the F2 layer, $f_H \leq$ foF2 and above foF2, $f_H >$ foF2 [*Blagoveshchenskaya et al*., 2014; 2015].

To summarize, the comparison between the X- and O-mode plasma and ion line spectra derived with 5 s resolution clearly exhibits the radical differences that allows us to distinguish correctly the HF-enhanced plasma and ion lines (HFPLs and HFILs) excited by the X- and O-mode HF pump waves.

3. The analysis of Wang et al. (2016) and where it fails

The flaws in the analysis of the parametric instability induced by X-mode HF pump wave by WANG2016 are now described step by step in the following section.

HFPLs and HFILs excited by O- and X-mode pump waves cannot be separated in EISCAT UHF radar spectra.

Comment: We propose you can distinguish the O- and X-mode effects according to the behavior in time after the onset of HF pumping and specific features of the HF-enhanced plasma and ion line spectra. The radical difference between the X- and O-mode plasma and ion line spectra derived with 5 s resolution was clearly demonstrated in Section 2 and Figs. 2 - 7. Namely, under O-mode HF pumping the abrupt enhancements in the ion and plasma line power in spectra appeared from the "cold" start just immediately after the onset of HF heating and were seen in the first 5 s radar data dump. Thereafter Langmuir and ion-acoustic waves are normally quenched by fully generated artificial small-scale field-aligned irregularities (FAIs) preventing further generation of the PDI [*Stubbe*, 1996]. However, under high effective radiated power the reappearance of enhanced ion and plasma lines can occur after overshoots. Such a situation was observed during the O-mode pump pulse at f_H = 7.1 MHz when HF-enhanced upshifted and downshifted ion lines reappeared (see Fig. 2a, top panel and Fig. 4a).

The X-mode ion and plasma lines developed with a time delay relative to the onset of HF heating. After appearance, their intensity gradually increased and reached a maximum within about 1 min or even longer. Plasma and ion line backscatter, coexisting with the strong artificial field-aligned irregularities, were observed through the whole transmission pulse [*Blagoveshchenskaya et al*., 2014; 2015].

The leakage to O-mode wave at least 2% - 3% ERP under X-mode heating in the course of the experiment on October 22, 2013.

Comment: In the course of the experiment on October 22, 2013 the effective radiated power of the X-mode wave varied between 540 and 548 MW with peak gain at azimuth Az 180° and Zen 12° (transmission was produced to the magnetic zenith, MZ). The leakage to O-mode was about 10 MW with peak gain at Az 359° and Zen 27°. It means that the transmission of the O-mode wave occurred to the northward direction under low elevation angles, but not to the MZ, confirming that the leakage effect did not exceed 1%.

The HFILs and HFPLs excited by O- or X-mode cannot be separated in the spectrum due to the power leakage problem.

Comment: The power leakage effect to O-mode wave in the course of the X-mode HF heating can be easily recognized from the growth time and specific features of the plasma and ion line spectra. Even if the power leakage is enough to exceed the excitation threshold of the PDI, the abrupt enhancements in the ion and plasma line power in spectra would appear just immediately after the onset of HF heating in the first 5 s radar data dump. In the next few 5 s radar data dumps they are quenched by fully generated FAIs. If the leakage effect is negligibly small, we would expect the appearance of the X-mode plasma and ion line with a time delay relative to the onset of HF heating. After appearance their power would gradually enhance, reaching a maximum within about 1 min.

The parametric instability excited by O/X-mode pump wave in the course of the X-mode heating can be distinguished according to the different excitation heights.

Comment: WANG2016 separated the O- and X-mode effects according to the height of the reflection for O-and X-mode waves taken from ionograms recorded between heater pulses. In the course of the X-mode experiment on October 22, 2013 (case 1 by WANG 2016) downshifted HF-enhanced ion lines were excited at two different altitudes. They concluded that two downshifted HFILs at different heights were produced by the X- and O-mode pump waves.

Because of that they attributed the downshifted ion line at the O-mode reflection height to the small leakage to the O-mode during X-mode heating. As shown in Section 2, in this case the O-mode typical features should be observed near the reflection altitude in the first 5 s radar data dump (see Fig. 2a, 3a, and 4a). The simultaneous appearance of two downshifted ion lines at different altitudes is a typical feature in a large number of our EISCAT X-mode experiments carried out both at pump frequencies f_H < foF2 and f_H > foF2 [*Blagoveshchenskaya et al*., 2014; 2015]. In the latter case even the small O-mode leakage is completely excluded.

However, the analysis of the 5 s UHF radar plasma and ion line spectra on October 22, 2013 clearly revealed features typical for X-mode pumping (see Fig. 7 in Section 2).

It is important that the excitation of the PDI and /or OSTI requires a parallel electric field of the HF pump wave near the reflection altitude. However, the electric field of an X-mode wave is perpendicular to the magnetic field. We could suggest that some effective mechanism at the reflection height of the X-mode wave is acting, providing the conversion of the transverse electric field into the parallel one. For example, *Fejer and Leer* [1972] suggested that an exciting X-mode HF pump wave at the reflection height could be converted into the excited O-mode electromagnetic wave through the electromagnetic instability. Other conversion mechanisms could also act during the X-mode heating. More careful studies, both theoretical and experimental, are required in order to find out the mechanisms of the partial conversion of the transverse electric field of the X-mode pump wave into the parallel electric field. The excited wave with the parallel electric field can penetrate to the transformation point near the O- or Z-mode reflection altitude and produce PDI / OTSI.

The analysis of alternating O/X-mode experiment on October 19, 2012 (case 2 from WANG2016).

Comment: The Figure 2 by WANG2016 is not consistent with observational facts. Overview of the undecoded downshifted plasma line power and backscatter power (raw electron

density) obtained from the EISCAT UHF “raw” radar data with 20 s integration time in the course of the alternating O/X-mode heating experiment on October 19, 2012 from 17 to 19 UT clearly demonstrated the appearance of HF-enhanced ion and plasma lines for every O- and X-mode pulse except the last O-mode heater pulse from 18:46 – 18:56 UT. It is important that in the course of every transmission pulse the UHF radar was scanned in elevation angle between 76 – 80° with 1° steps every two minutes. The strongest HFPLs and HFILs were observed in the vicinity of the magnetic field-aligned direction at Tromsø (77-79°). At pump frequency f_H = 6.2 MHz the enhanced backscatter was observed in every transmission pulse. To the end of the O-mode pump pulse from 17:31 – 17:41 UT the heater wave penetrated out the ionosphere, but in the next X-mode pulse from 17:46 – 17:56 UT, when f_H exceeded the critical frequency foF2 (f_H > foF2), sufficiently strong enhanced plasma and ion lines were excited near magnetic zenith (77 - 79°). At pump frequency f_H = 5.423 MHz relatively strong HFILs and HFPLs were excited during the X-mode pulse from 18:01 – 18:11 UT and much weaker signatures only near the magnetic zenith can be seen from 18:31 – 18:41 UT. The O-mode HF pump wave penetrated out the ionosphere during the cycle from 18:16 – 18:26 UT. What is revealed from Figure 2 by WANG2016? They found the only X-mode transmission pulse in which HF-enhanced plasma and ion lines were observed. However, the HFILs were also observed in the preceding O-mode pulse that is not shown in Figure 2 by WANG 2016. The comparison between the O- and X-mode effects and the excitation of the PDI and OTSI near the reflection altitude of the X-mode HF pump wave for the same pump pulses has already been shown by *Blagoveshchenskaya et al.* [2014].

The O-mode HF pump wave penetrates out the ionosphere according to the ionosonde records (Case 3 by WANG2016).

Comment: In the course of the experiment on February 21, 2013 the HF-enhanced plasma and ion lines at pump frequency of 7.1 MHz were produced by both the O- and X-mode HF

pump wave, as shown in Section 2 and Fig. 1. Thus, the O-mode wave was certainly reflected from the ionosphere. This confirms that reflection altitudes of the O-and X-mode waves, obtained from the ionosonde records between the transmission pulses, whilst it provides a rough measure of such altitudes, can be incorrect, and cannot be used for the separation of the O- and X-mode effects.

Strong HF-induced plasma and ion lines at pump frequency of 7.1 MHz were observed near the reflection height of the X-mode wave (Case 3 by WANG2016).

Comment: It is not evident at what altitudes they were excited. In Section 2 we presented results of the analysis in detail and comparison between plasma and ion line spectra derived from "raw" UHF radar data with 5 s time resolution, excited by O- and X-mode heating wave at pump frequency of f_H = 7.1 MHz (see also Figs. 2a, 3 and 4). As seen from Fig. 3, the X-mode downshifted plasma line spectrum appeared within 15 s after the onset of HF pumping (T_0) at an altitude of 225 km, which is 3 km higher as compared with the initial appearance of the O-mode plasma line spectrum in the first 5 s radar data dump. The X-mode ion line spectrum, similar to the plasma line spectra, also appeared within 15 s after T_0 at the same altitudes as the O-mode ion line spectrum in the first 5 s radar data dump (see Fig. 4). Therefore it is not possible to separate the O- and X-mode effects according their reflection heights from ionosonde records between heater pulses as was done by WANG2016. However, the evolution in time of enhanced plasma and ion line spectra after T_0 and their spectral features, provide sufficient evidence to clearly distinguish the O-and X-mode effects.

Ascending and descending HFPL and HFIL echoes observed at X-mode heating (Case 3 by WANG2016).

Comment: Ascending and descending echoes of the HFPLs and the HFILs by WANG2016 observed at X-mode heating periods from 13:16 - 13:26 UT and 13:46 - 13:56 UT,

were caused by background ionospheric changes. From 13:16 - 13:26 UT the background ionosphere dropped and reflection altitudes increased. In the course of the pump pulse from 13:46 - 13:56 UT the background ionosphere enhanced and reflection altitudes decreased. This has nothing to do with descending structures observed at the EISCAT/Heating and HAARP under O-mode pumping which were reported and discussed by *Dhillon and Robinson* [2005], *Ashrafi et al.* [2007], and *Mishin et al*. [2016]. However, such descending ion line backscatter was observed at O-mode pumping at pump frequencies of 7.1 and 5.423 MHz on February 21, 2013 and clearly recognized from Figs. 4 and 6 in Section 2.

The absence of HFPLs at O-mode pumping (case 3 by WANG2016).

Comment: Such statement is incorrect. The intense HF-enhanced plasma lines under O-mode heating at frequencies of 7.1 and 5.423 MHz were observed in the first 5 s UHF radar dump as shown in section 2 (see Fig. 2a and b, top panels, and Figs. 3a and 5a).

The electron temperature increased in every transmission pulse (Case 3 by WANG2016).

Comment: Intense HF-enhanced ion lines were excited through the experiment on February 21, 2016. This does not make it possible to perform the proper estimations of the electron temperature (Te) at the resonance altitude due to a high residual to the fitting. Estimations of Te in the course of the alternating O/X-mode EISCAT heating experiment, when HFILs were not excited, were performed by *Blagoveshchenskaya et al*. [2015]. It was shown that under X-mode heating the Te increases were weak (about 20 % above the background values), when the heater frequency was below the critical frequency foF2, and increased up to 50%, when f_H exceeded foF2. At the same time the O-mode heating demonstrated very strong Te increases up to 300 %, when $f_H \leq$ foF2.

Figure 3 demonstrates the behavior of HFPLs and HFILs in the course of alternating O/X-mode heating experiment on February 21, 2013 (Case 3 by WANG2016).

Comment: The Figure 3 by WANG2016 is not consistent with observational facts (see comments above for Case 3 by WANG2016).

Table 1 summarizes the parametrically excited plasma waves observed in three cases.

Comment: The presence of downshifted HFPLs, upshifted, downshifted, and zero-offset ion lines in Table 1 is incorrect (see all comments above and Section 2).

The parallel electric field threshold for PDI and OTSI excitation.

Comment: Equations (9) and (10) by WANG2016 are appropriate to the case of "classic" resonance parametric decay instability / oscillating two-stream instability excited from the "cold" start as an immediate response to the pumping onset and seen as overshoot in the first few radar data dumps. Thereafter Langmuir and ion-acoustic waves are normally quenched by fully generated FAIs preventing further generation of PDI [*Stubbe*, 1996]. It is realized under O-mode HF pumping at heater frequencies $f_H \leq foF2$. It is important that the O-mode FAIs at EISCAT were generated for effective radiated power ERP < 4 MW O-mode waves [*Wright et al.*, 2006].

The radically different behavior of the persistent Langmuir and ion-acoustic waves are typical for the X-mode HF pumping. They are excited, both at $f_H \leq foF2$ and $foF2 < f_H \leq fxF2$, not from the "cold' start, their intensity gradually enhanced reaching a maximum within 1 min. This clearly demonstrates the other type of the parametric instability which, most likely, could be of non-resonance type and requires higher electric field threshold. More careful studies, both theoretical and numerical, are needed in order to detail the processes and mechanisms of the partial conversion of the X-mode into O- and Z-mode. How the parallel component of the electric field under X-mode heating is generated, however, is not discussed and explained. Unfortunately, besides of the leakage to O-mode, results by WANG2016 do not explain the

potential mechanisms for PDI and OTSI and don't add any ideas to understanding the physical factors accounting for parametric instability generated by an X-mode HF pump wave.

Thresholds of the parallel electric field for the PDI and OTSI excitation in Table 2.

Comment: Thresholds derived from Eq. (9) and (10) would hold for the classic resonance PDI and OTSI excited as immediate response to the onset of heating (overshoot in the first few 5 s radar data dumps) and are typical only for O-mode pumping at $f_H \leq foF2$. The same is true for Figure 4 by WANG 2016.

4. Summary

By analyzing the observations from EISCAT, WANG2016 claim to explain the potential mechanisms for parametric decay instability (PDI) and oscillating two-stream instability (OTSI) and to understand the physical factors accounting for parametric instability generated by an X-mode HF pump wave. Their analysis of the EISCAT observations is flawed, and their conclusions are based on the incorrect separation of the X- and O-mode effects. The serious limitation in their analysis and interpretation of the PDI/OTSI is the use of 30 s integration time of the UHF radar data.

The analysis fails to the following specific reasons:

(1) WANG2016 claim that HF-enhanced plasma and ion lines (HFPLs and HFILs) excited by O- and X-mode pump waves cannot be separated in the EISCAT UHF radar spectra. The fact is, however, that there is a radical difference between the X- and O-mode plasma and ion line spectra derived with 5 s resolution and their growth time after the onset of HF pumping. That provides the correct separation of the X- and O-mode effects.

(2) The leakage to the O-mode wave in the course of the X-mode experiment on October 22, 2013 was estimated by 2-3%, but the real leakage is certainly less by 1% taking into account the direction of the leakage power radiation. Moreover, even if the power leakage is enough to

exceed the PDI excitation threshold, the specific changes in the plasma and ion line spectra typical for O-mode heating which allow to correctly distinguish the O- and X-mode effects will occur. Analysis of the 5s UHF radar plasma and ion line spectra on October 22, 2013 clearly revealed features typical for X-mode pumping.

(3) WANG2016 distinguished the parametric instability excited by O- /X-mode heating waves according to the different excitation heights. The reflection altitudes were determined from the ionograms taken between heater pulses. However, this provides only a rough measure of altitudes, can be incorrect, and cannot be used for the separation of the O- and X-mode effects.

(4) Figures 2 and 3, Table 1 showing the results by WANG2016 on October 19, 2012 and February 21, 2013 are completely inconsistent with real observational facts of HF-enhanced plasma and ion lines (HFPLs and HFILs).

(5) WANG 2016 claim that the O-mode HF pump wave at pump frequency of 7.1 MHz penetrates the ionosphere according to the ionosonde records during the experiment on February 21, 2013 which, however, is not representative of the real ionosphere.

(6) WANG2016 claim that the HFPLs at O-mode pumping were not generated. The fact is, however, that very intense plasma line spectra were observed in the first 5 s EISCAT UHF radar dump both at frequencies of 7.1 and 5.423 MHz on February 21, 2013.

(7) They claimed that the strong HFPLs and HFILs at pump frequency of 7.1 MHz on February 21, 2013 were observed near the reflection height of the X-mode wave. However the fact is that the X-mode ion line spectrum appeared within 15 s after T_0 at the same altitude as the O-mode ion line spectrum in the first 5 s radar data dump.

(8) Ascending and descending echoes of the HFPLs and the HFILs, observed by WANG2016 at some X-mode heating periods on February 21, 2013 were caused by the background ionospheric changes. This has nothing to do with descending structures previously observed at the EISCAT/Heating and HAARP under O-mode pumping.

(9) WANG2016 state that the electron temperature increased in every transmission pulse in the course of the experiment on February 21, 2013. However, it is not possible to perform proper estimations of the electron temperature at the resonance altitude due to a high residual to the fitting induced by intense HF-enhanced ion lines excited through the experiment.

(10) Thresholds of the parallel electric field for the PDI and OTSI excitation derived by WANG2016 would hold for the classic resonance PDI and OTSI excited as immediate response to the onset of heating (overshoot in the first few 5 s radar data dumps) and are typical only for O-mode pumping at $f_H \leq$ foF2. Radically different behavior of the persistent Langmuir and ion-acoustic waves here are typical for the X-mode HF pumping excited, both at $f_H \leq$ foF2 and foF2< $f_H \leq$ fxF2. This clearly demonstrates the other type of the parametric instability which, most likely, could be of the non-resonance type.

(11) How the parallel component of the electric field under X-mode heating is generated, however, is not discussed and explained. Unfortunately, besides of the leakage to O-mode, results by WANG2016 do not explain the potential mechanisms for PDI and OTSI and do not add any ideas to understanding the physical factors accounting for parametric instability generated by an X-mode HF pump wave.

In short, the analysis of the parametric decay instability by WANG2016 is flawed. Their separation of O- and X mode effects is incorrect. However, the separation of the O- and X-mode effects plays a crucial role in further analysis of the parametric decay instability (PDI). The further analysis by WANG2016 fails if such separation is incorrect. Results by WANG2016 do not explain the potential mechanisms for PDI and OTSI and do not add any ideas to understanding the physical factors accounting for parametric instability generated by an X-mode HF pump wave.

Acknowledgements. EISCAT is an international scientific association supported by research organizations in China (CRIRP), Finland (SA), Japan (NIPR and STEL), Norway (NFR), Sweden (VR), and the United Kingdom (NERC). TKY is supported by Science and Technology Facilities Council Grant ST/H002480/1. The data used in this comment are available through the EISCAT Madrigal database (http://www.eiscat.se/madrigal/).

References

Ashrafi, M., M. J. Kosch, K. Kaila, and B. Isham (2007), Spatiotemporal evolution of radio wave pump-induced ionospheric phenomena near the fourth electron gyroharmonic, *J. Geophys. Res., 112*, A05314, doi:10.1029/2006JA011938.

Blagoveshchenskaya, N. F., T. D. Borisova, T. K. Yeoman, and M. T. Rietveld (2011a.), The effests of modification of a high-latitude ionosphere by high-power HF radio waves. Part 1. Results of multi-instrument ground-based observations, *Radiophys. Quant. Electron*. (Engl. Transl.), *53*, (9-10), 512 – 531.

Blagoveshchenskaya, N. F., T. D. Borisova, T. Yeoman, M. T. Rietveld, I. M. Ivanova, and L .J. Baddeley (2011b), Artificial field-aligned irregularities in the high-latitude F region of the ionosphere induced by an X-mode HF heater wave, *Geophys. Res. Lett*., *38*, L08802, doi: 10.1029/2011GL046724.

Blagoveshchenskaya, N. F., T. D. Borisova, T. K. Yeoman, M. T. Rietveld, I. Häggström, and I. M. Ivanova (2013), Plasma modifications induced by an X-mode HF heater wave in the high latitude F region of the ionosphere, *J. Atmos. Sol. Terr. Phys., 105-106*, 231 - 244.

Blagoveshchenskaya, N. F., T. D. Borisova, M. Kosch, T. Sergienko, U. Brändström, T.K., Yeoman, and I. Häggström (2014), Optical and Ionospheric Phenomena at EISCAT under Continuous X-mode HF Pumping, *J. Geophys. Res. Space Physics*, *119*, 10,483–10,498, doi:10.1002/ 2014JA020658.

Blagoveshchenskaya, N.F., T.D. Borisova, T.K. Yeoman, I. Häggström, and A.S. Kalishin (2015), Modification of the high latitude ionosphere F region by X-mode powerful HF radio waves: Experimental results from multi-instrument diagnostics, *J. Atmos. Sol.-Terr. Phys., 135*, 50–63.

Dhillon, R. S., and T. R. Robinson (2005), Observations of time dependence and aspect sensitivity of regions of enhanced UHF backscatter associated with RF heating, *Ann. Geophys., 23*, 75–85.

DuBois, D. F., H. A. Rose, and D. Russell (1990), Excitation of strong Langmuir turbulence in plasmas near critical density: Application to HF heating of the ionosphere, *J. Geophys. Res*., *95*, 21221 – 21272.

Fejer, J. A. and E. Leer (1972), Excitation of parametric instabilities by radio waves in the ionosphere, *Radio Sci., 7*(4), 481-491.

Fejer, J.A. (1979), Ionospheric Modification and Parametric Instabilities, *Rev. Geophys. Space Phys.*, *17* (1), 135 - 153.

Gurevich, A.V., H. C. Carlson, Yu.V. Medvedev, and K. R. Zybin (2004), Langmuir turbulence in ionospheric plasma, *Plasma Phys. Rep*., *30*, 995 - 1005.

Hagfors, T., W. Kofman, H. Kopka, P. Stubbe, and T. Ijnen (1983), Observations of enhanced plasma lines by EISCAT during heating experiments, *Radio Sci*., *18*, 861 – 866.

Kuo, S., M. Lee, and P. Kossey (1997), Excitation of oscillating two stream instability by upper hybrid pump in ionospheric heating experiments at Tromsø, *Geophys. Res. Lett.*, *24*, 2969 - 2972.

Kuo, S. (2015), Ionospheric modifications in high frequency heating experiments, *Phys. Plasmas, 22*, 012901, doi: 10.1063/1.4905519.

Mishin, E., B. Watkins, N. Lehtinen, B. Eliasson, T. Pedersen, and S. Grach (2016), Artificial ionospheric layers driven by high-frequency radiowaves: An assessment, *J. Geophys. Res. Space Physics*, *121*, doi:10.1002/2015JA021823.

Perkins, F.W., C. Oberman, and E.J. Valco (1974), Parametric instabilities and ionospheric modification, *J. Geophys. Res*., *79*, 1478 – 1496.

Robinson, T.R. (1989), The heating of the high latitude ionosphere by high power radio waves, *Phys. Rep*., *179*, 79 - 209.

Sharma, R. P., A. Kumar, R. Kumar, and Y.K. Tripathi (1994), Excitation of electron Bernstein and ion Bernstein waves by extraordinary electromagnetic pump: Kinetic theory, *Phys. Plasmas. 1*(3), 522 – 527, DOI:10.1063/1.870796.

Stubbe, P., H. Kohl, and M.T. Rietveld (1992), Langmuir turbulence and ionospheric modification, *J. Geophys. Res*., *97*, 6285 - 6297.

Stubbe P. (1996), Review of ionospheric modification experiments at Tromso, *J. Atmos. Terr. Phys.*, *58*, 349 – 368.

Vas'kov, V. V., and N. A. Ryabova (1998), Parametric excitation of high frequency plasma oscillations in the ionosphere by a powerful extraordinary radio wave, *Adv. Space Res*., *21*, 697 - 700

Wang, X., C. Zhou, M. Liu, F. Honary, B. Ni, and Z. Zhao (2016), Parametric Instability Induced by X-Mode Wave Heating at EISCAT, *J. Geophys. Res. Space Phys.*, *121*, 10,536 – 10,548, doi: 10.1002/2016JA023070.

Wright, D. M., J. A. Davies, T. K. Yeoman, T. R. Robinson, and H. Shergill (2006), Saturation and hysteresis effects in ionospheric modification experiments observed by the CUTLASS and EISCAT radars, *Ann. Geophys*., *24*, 543–553, 2006

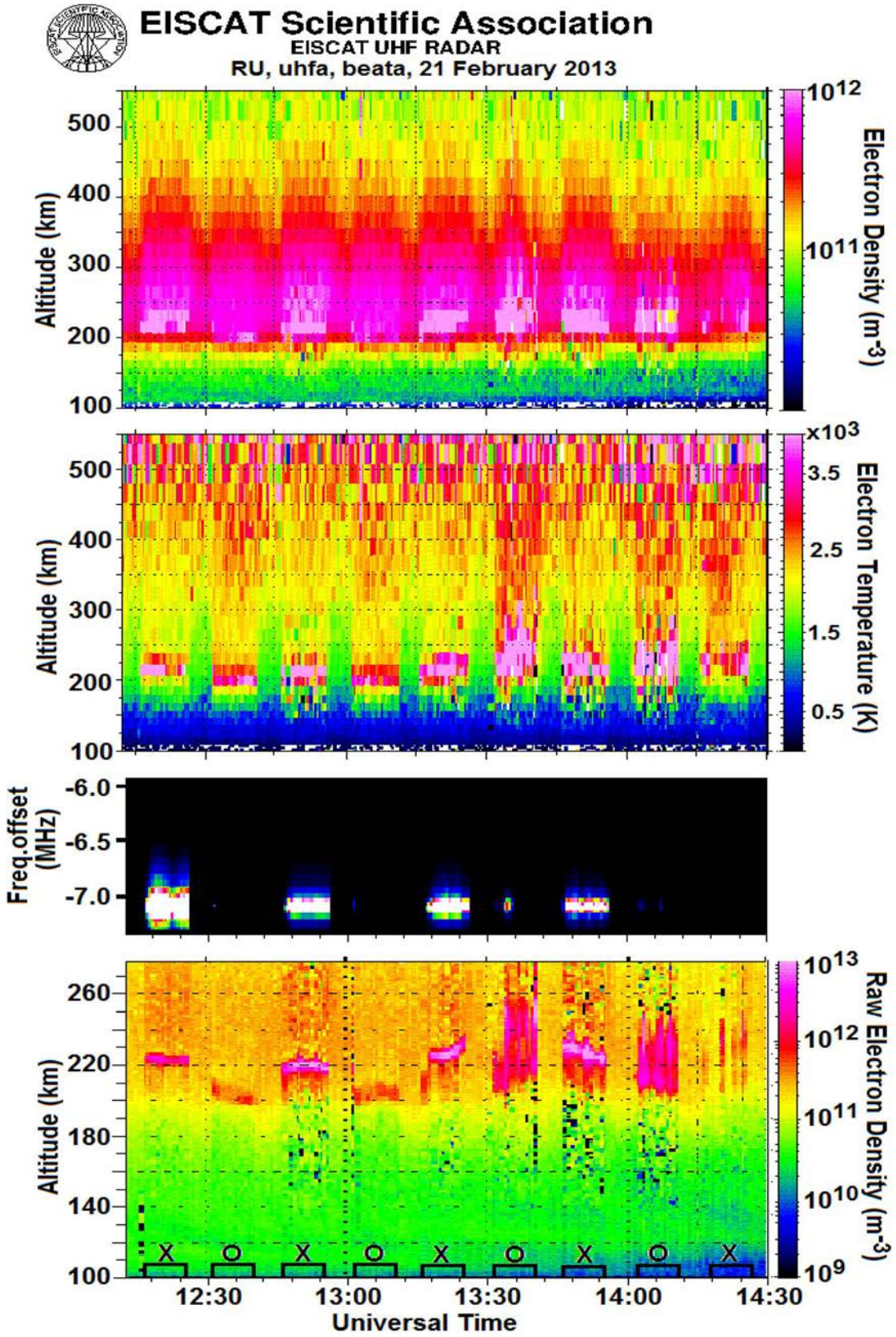
EISCAT Scientific Association
EISCAT UHF RADAR
RU, uhfa, beata, 21 February 2013
Altitude (km)
Electron Density (m-3)
Electron Temperature (K)
x103
Freq.offset (MHz)
Raw Electron Density (m-3)
Universal Time
12:30
13:00
13:30
14:00
14:30

Figure 1. The behavior of the electron density (Ne) and temperature (Te), undecoded downshifted plasma line power in the altitude range of 128 – 302 km, and the raw electron density (backscattered power) from EISCAT UHF radar measurements with 30 s integration time during alternating O/X-mode EISCAT HF heating experiment on February 21, 2013 from 12:12 – 14:30 UT. HF pumping was produced towards the magnetic zenith with the effective radiated power of about 530 MW at heater frequency of 7.1 MHz by 10 min on, 5 min off pulses. The HF pump pulses and polarization of the heater wave are shown on the time axis.

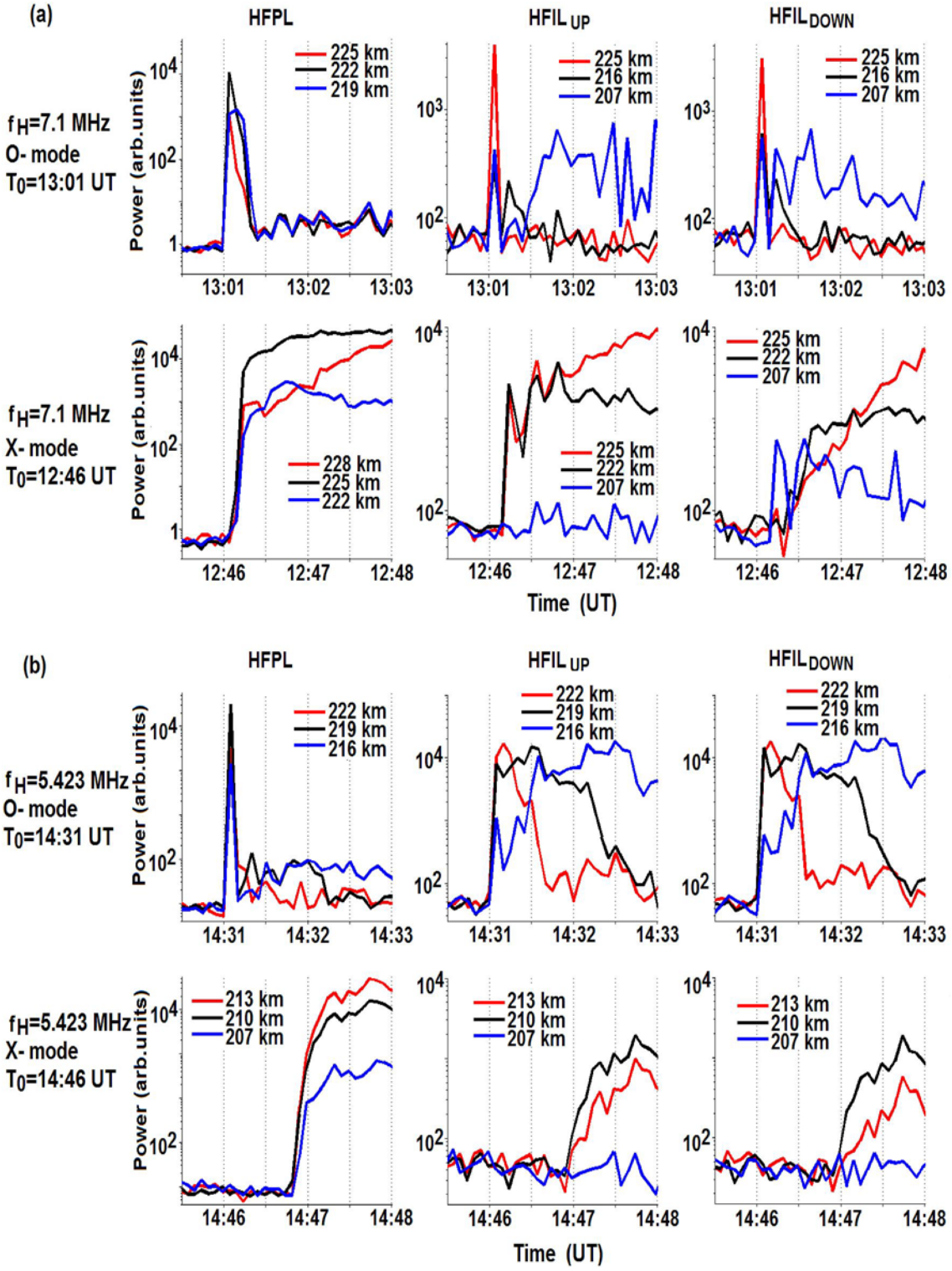
(a)
HFPL
HFIL UP
HFIL DOWN
fH=7.1 MHz
O- mode
T0=13:01 UT
225 km
222 km
219 km
225 km
216 km
207 km
225 km
216 km
207 km
Power (arb.units)
13:01
13:02
13:03
fH=7.1 MHz
X- mode
T0=12:46 UT
228 km
225 km
222 km
225 km
222 km
207 km
225 km
222 km
207 km
12:46
12:47
12:48
Time (UT)
(b)
HFPL
HFIL UP
HFIL DOWN
fH=5.423 MHz
O- mode
T0=14:31 UT
222 km
219 km
216 km
222 km
219 km
216 km
222 km
219 km
216 km
14:31
14:32
14:33
fH=5.423 MHz
X- mode
T0=14:46 UT
213 km
210 km
207 km
213 km
210 km
207 km
213 km
210 km
207 km
14:46
14:47
14:48
Time (UT)

Figure 2. The maximum power of HF-enhanced downshifted plasma lines (HFPL), upshifted ($HFIL_{UP}$) and downshifted (HF_{DOWN}) ion lines at three fixed altitudes during 30 s before and the first two min of the pump pulse for O- and X-mode pulses obtained from EISCAT UHF radar measurements on February 21, 2013. (a) Heater frequency of 7.1 MHz; (b) Heater frequency of 5.423 MHz. The power of the HFPLs and HFILs was found as the maximum in spectra derived every 5 s with 3 km altitude steps. T_0 denotes the onset of the transmission pulse.

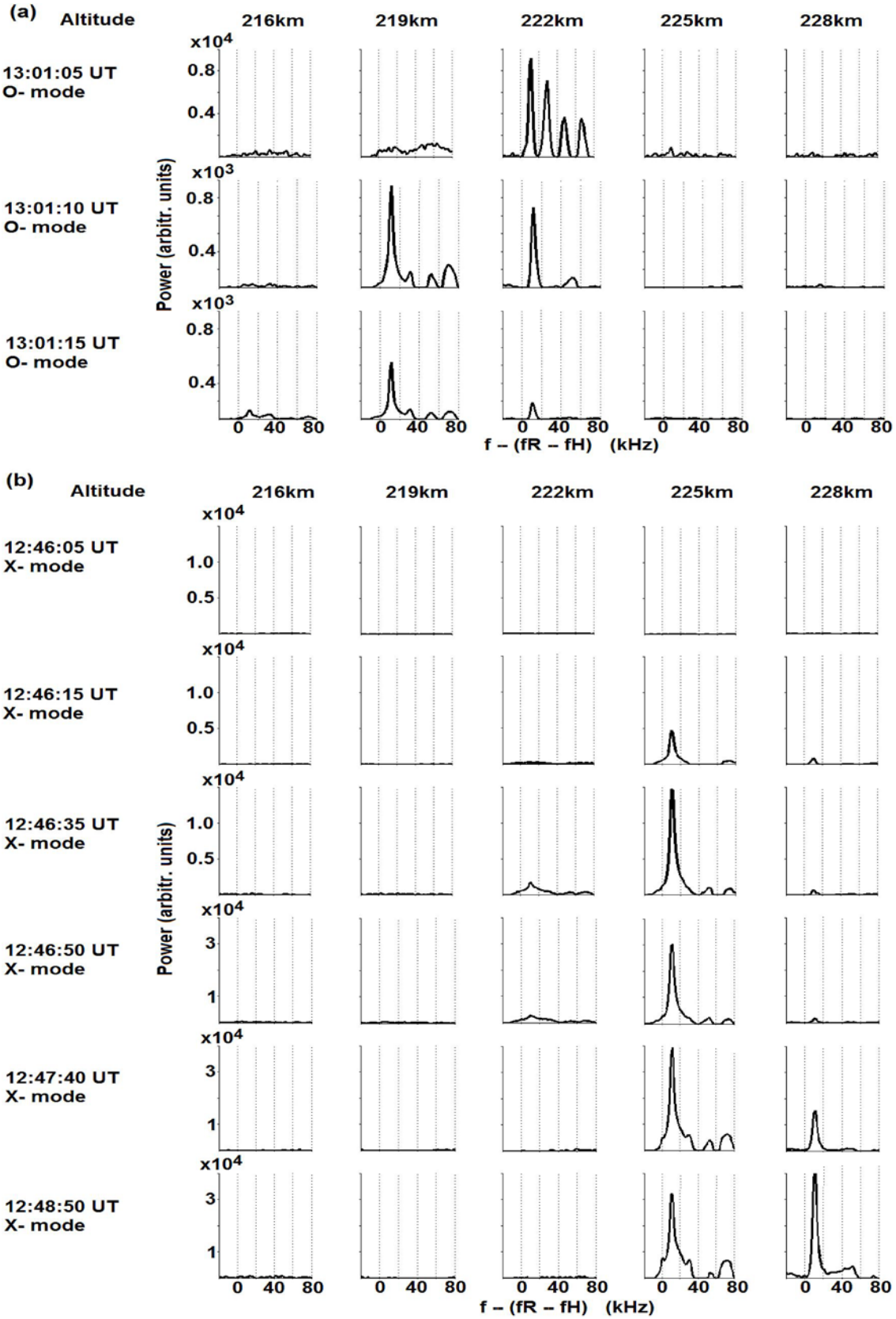
(a)
Altitude
216km
219km
222km
225km
228km
13:01:05 UT
O- mode
13:01:10 UT
O- mode
13:01:15 UT
O- mode
x10^4
x10^3
0.8
0.4
Power (arbitr. units)
0
40
80
f – (fR – fH) (kHz)
(b)
Altitude
216km
219km
222km
225km
228km
12:46:05 UT
X- mode
12:46:15 UT
X- mode
12:46:35 UT
X- mode
12:46:50 UT
X- mode
12:47:40 UT
X- mode
12:48:50 UT
X- mode
x10^4
1.0
0.5
3
1
Power (arbitr. units)
0
40
80
f – (fR – fH) (kHz)

Figure 3. The downshifted plasma line spectra derived from the EISCAT UHF “raw” data with 5 s resolution in time at five fixed altitudes for different times after the onset of HF pumping taken on February 21, 2013 at heater frequency f_H = 7.1 MHz. (a)The O-mode transmission pulse with the onset at 13:01:00 UT. The scale of power was changed at 13:01:10 UT due to the strong decrease of the intensity of the downshifted plasma line spectra. (b) The X-mode pulse with the onset at 12:46:00 UT. The scale of power was changed at 12:46:50 UT due to the strong increase of the intensity of the downshifted plasma line spectra.

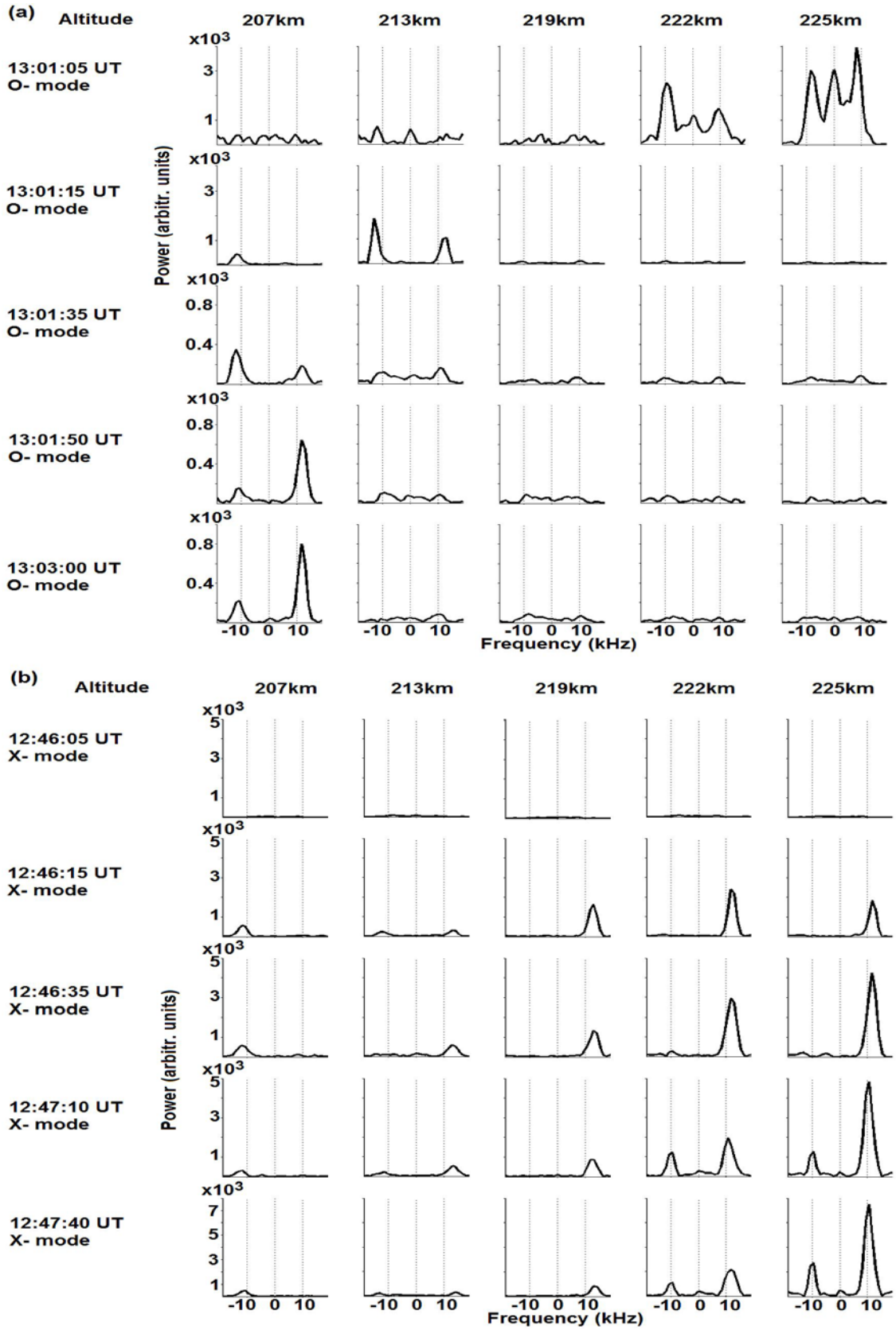
(a)
Altitude
207km
213km
219km
222km
225km
13:01:05 UT
O- mode
13:01:15 UT
O- mode
13:01:35 UT
O- mode
13:01:50 UT
O- mode
13:03:00 UT
O- mode
Power (arbitr. units)
x10^3
Frequency (kHz)
(b)
Altitude
207km
213km
219km
222km
225km
12:46:05 UT
X- mode
12:46:15 UT
X- mode
12:46:35 UT
X- mode
12:47:10 UT
X- mode
12:47:40 UT
X- mode
Power (arbitr. units)
x10^3
Frequency (kHz)

Figure 4. The ion line spectra derived from the EISCAT UHF “raw” data with 5 s temporal resolution at five fixed altitudes for different times after the onset of HF pumping taken on February 21, 2013 at heater frequency f_H = 7.1 MHz. (a) The O-mode transmission pulse with the onset at 13:01:00 UT. The scale of power was changed at 13:01:35 UT due to the decrease of the intensity of the downshifted plasma line spectra. (b) The X-mode pulse with the onset at 12:46:00 UT. The scale of power was changed at 12:47:40 UT due to the increase of the intensity of the downshifted plasma line spectra.

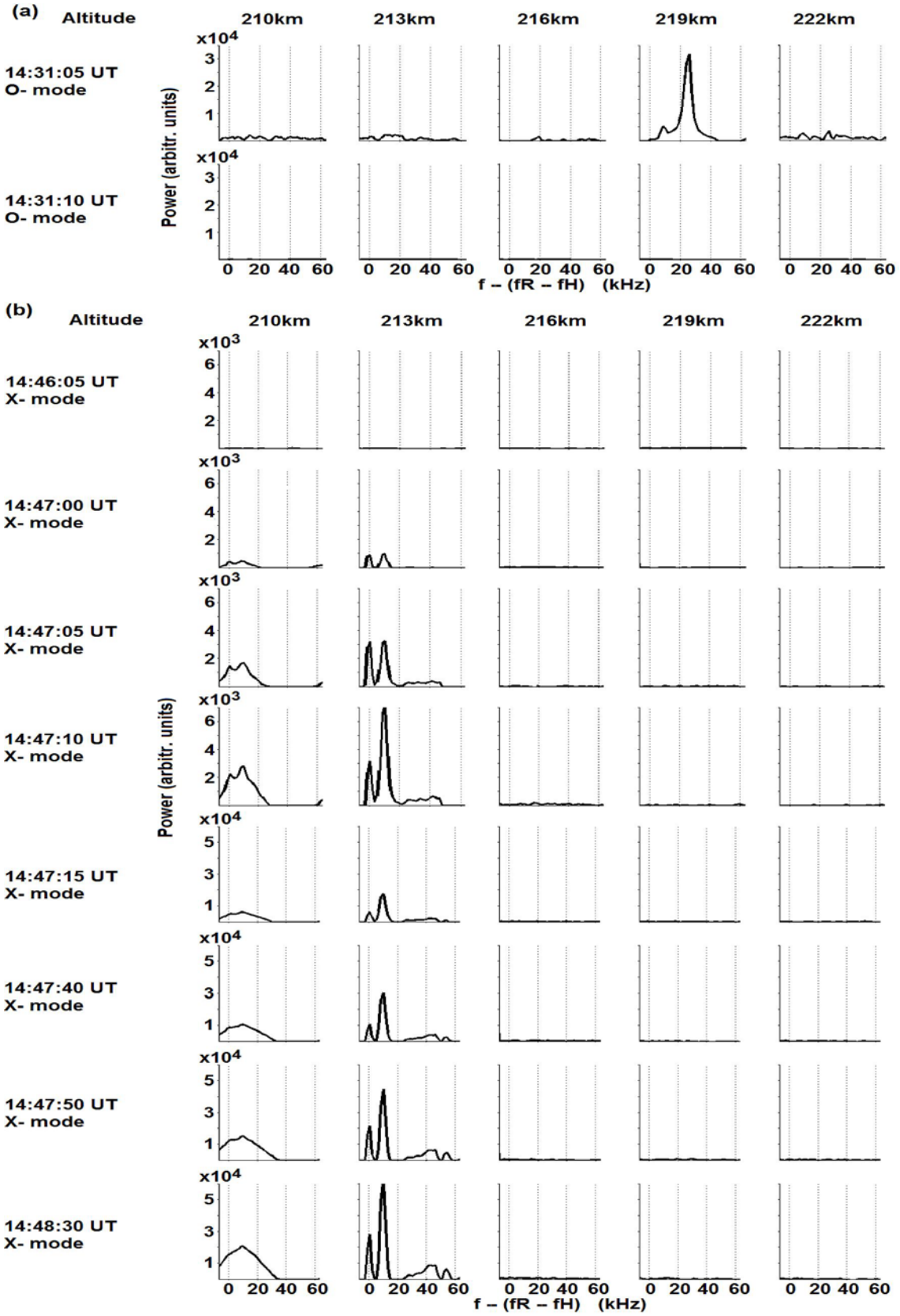
(a)
Altitude
210km
213km
216km
219km
222km
14:31:05 UT
O- mode
14:31:10 UT
O- mode
x10^4
Power (arbitr. units)
0 20 40 60
f – (fR – fH) (kHz)
(b)
Altitude
210km
213km
216km
219km
222km
14:46:05 UT
X- mode
14:47:00 UT
X- mode
14:47:05 UT
X- mode
14:47:10 UT
X- mode
14:47:15 UT
X- mode
14:47:40 UT
X- mode
14:47:50 UT
X- mode
14:48:30 UT
X- mode
x10^3
x10^4
Power (arbitr. units)
0 20 40 60
f – (fR – fH) (kHz)

Figure 5. The downshifted plasma line spectra derived from the EISCAT UHF “raw” data with 5 s temporal resolution at five fixed altitudes for different times after the onset of HF pumping taken on February 21, 2013 at heater frequency f_H = 5.423 MHz. (a) The O-mode transmission pulse with the onset at 14:301:00 UT. (b) The X-mode pulse with the onset at 14:46:00 UT. The scale of power was changed at 14:47:15 due to strong increase of the intensity of the downshifted plasma line spectra.

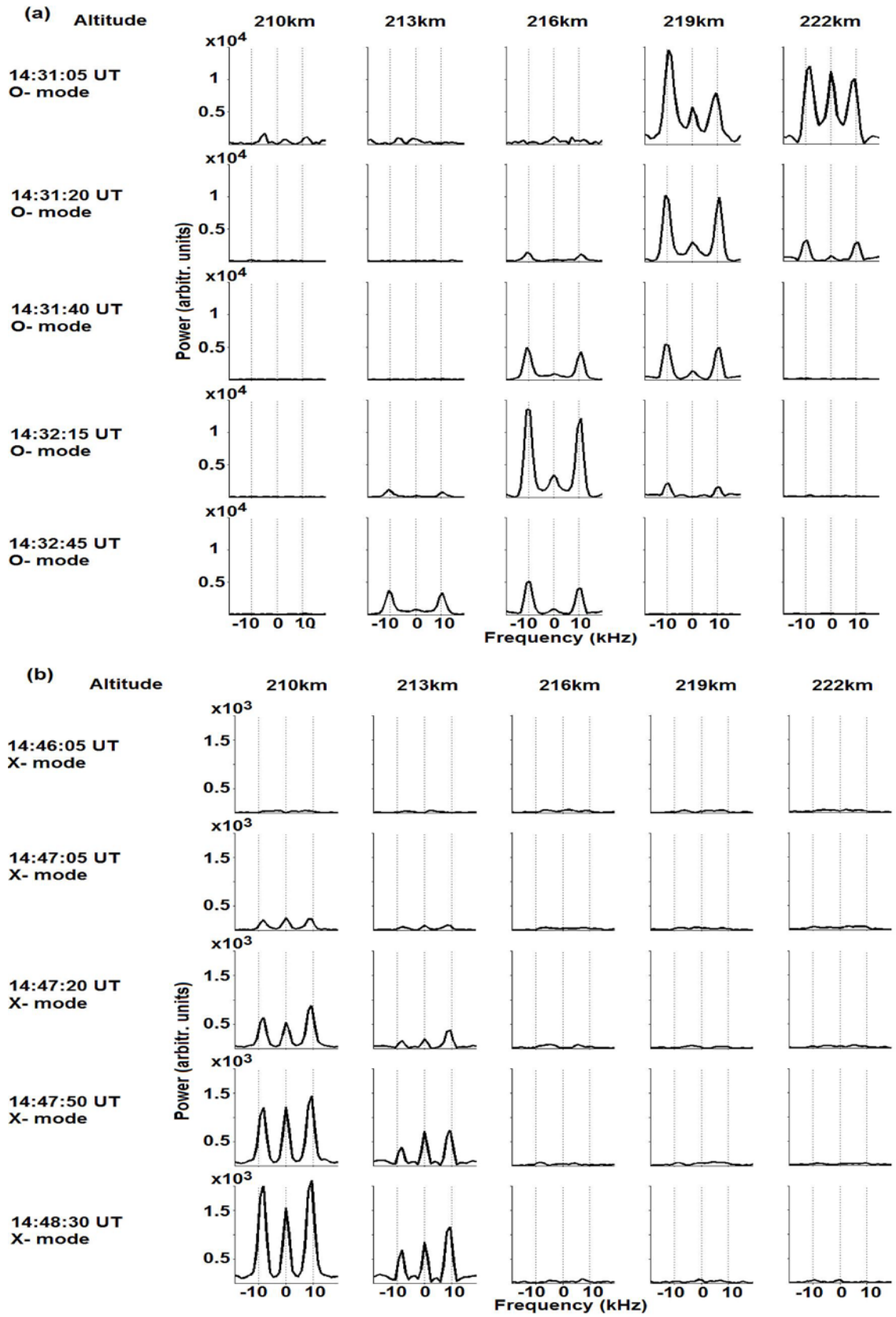
(a)
Altitude
210km
213km
216km
219km
222km
14:31:05 UT
O- mode
14:31:20 UT
O- mode
14:31:40 UT
O- mode
14:32:15 UT
O- mode
14:32:45 UT
O- mode
x10^4
1
0.5
Power (arbitr. units)
-10 0 10
Frequency (kHz)
(b)
Altitude
210km
213km
216km
219km
222km
14:46:05 UT
X- mode
14:47:05 UT
X- mode
14:47:20 UT
X- mode
14:47:50 UT
X- mode
14:48:30 UT
X- mode
x10^3
1.5
0.5
Power (arbitr. units)
-10 0 10
Frequency (kHz)

Figure 6. The ion line spectra derived from the EISCAT UHF “raw” data with 5 s temporal resolution at five fixed altitudes for different times after the onset of HF pumping taken on February 21, 2013 at heater frequency f_H = 5.423 MHz. (a) The O-mode transmission pulse with the onset at 14:31:00 UT. (b) The X-mode pulse with the onset at 14:46:00 UT.

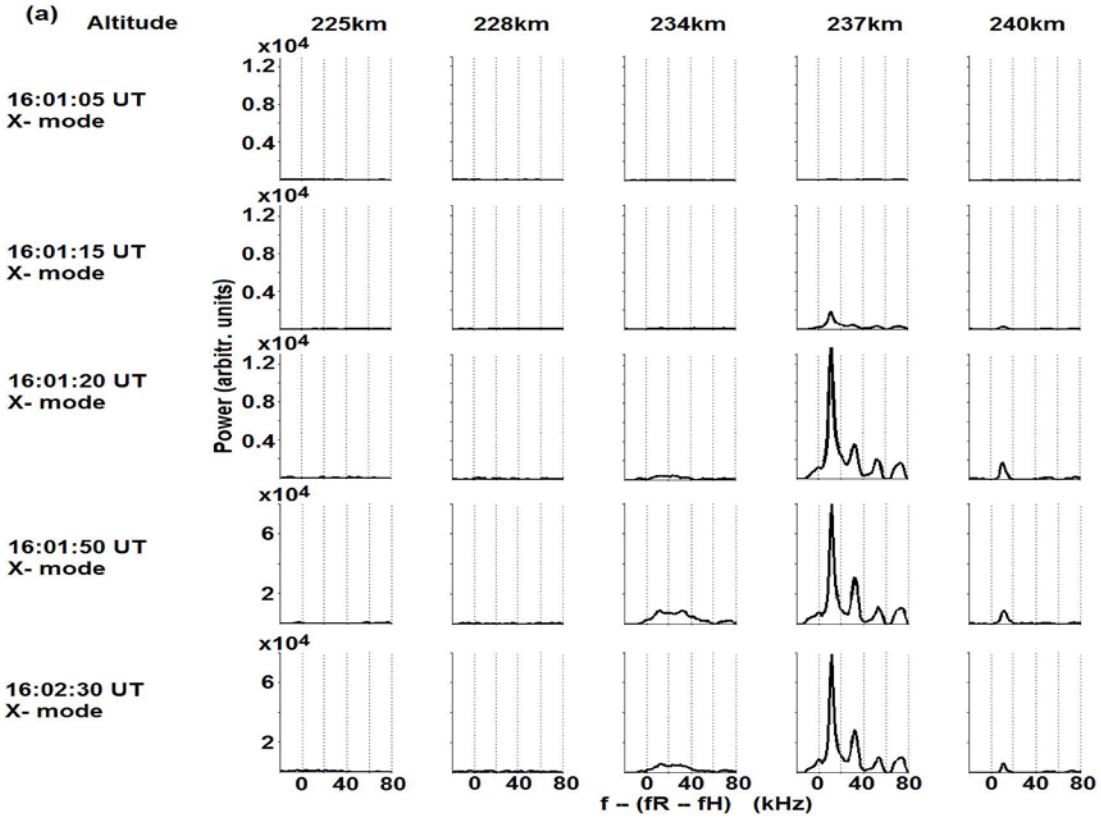
(a)
Altitude
225km
228km
234km
237km
240km
16:01:05 UT
X- mode
16:01:15 UT
X- mode
16:01:20 UT
X- mode
16:01:50 UT
X- mode
16:02:30 UT
X- mode
x10^4
Power (arbitr. units)
f – (fR – fH) (kHz)

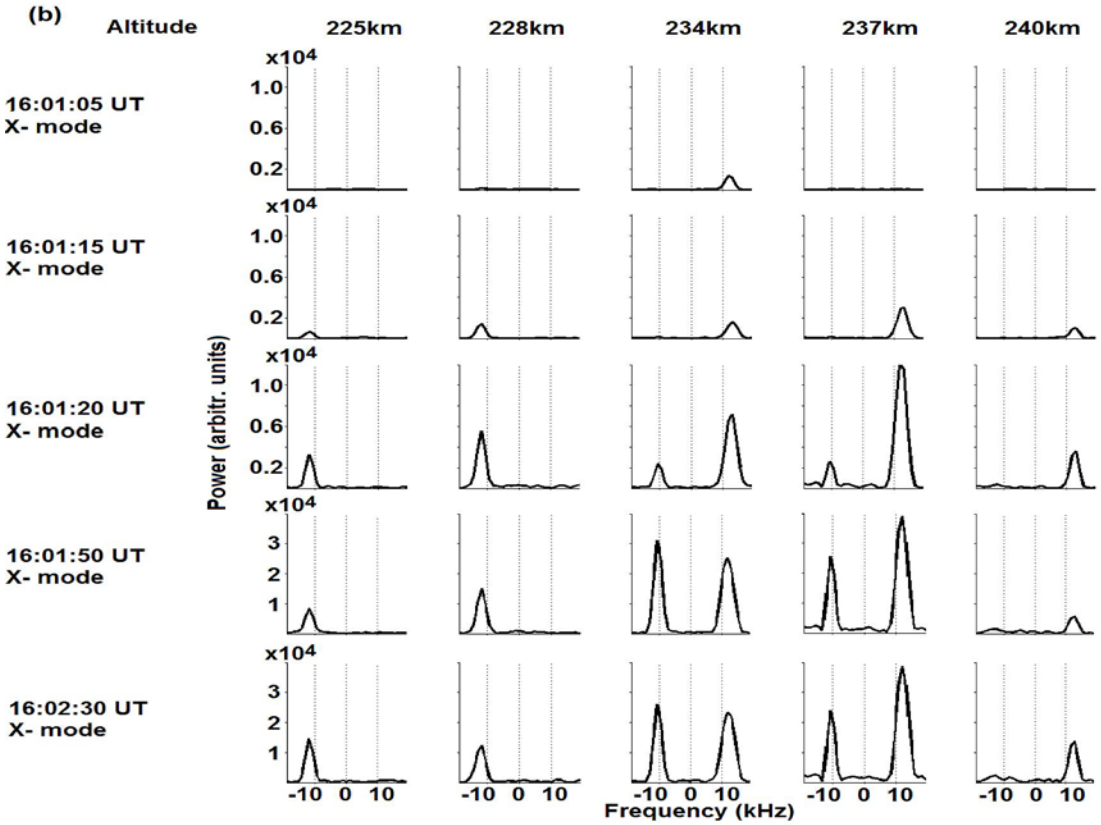
(b)
Altitude
225km
228km
234km
237km
240km
16:01:05 UT
X- mode
16:01:15 UT
X- mode
16:01:20 UT
X- mode
16:01:50 UT
X- mode
16:02:30 UT
X- mode
x10^4
Power (arbitr. units)
Frequency (kHz)

Figure 7. Plasma and ion line spectra derived from the EISCAT UHF “raw” data with 5 s resolution in time on October 22, 2013 at five altitudes for different times after the onset of the transmission pulse at heater frequency f_H = 7.1 MHz. (a) The downshifted plasma line spectra. (b) The ion line spectra. An extraordinary (X-mode) HF pump wave with the effective radiated power of about 550 MW was radiated towards the magnetic zenith from 16:01 – 16:11 UT. The scale of powers was changed at 16:01:50 UT due to strong increases of the power of plasma and ion line spectra.